

Supporting Information

Phomeroids A and B: Two Novel Cytotoxic Meroterpenoids from the Deep-Sea-Derived Fungus *Phomopsis tersa* FS441

Shanchong Chen,^{a,b} Zhaoming Liu,^a Haibo Tan,^c Yuchan Chen,^a Saini Li,^a Haohua Li,^a Shuang Zhu,^b Hongxin Liu,^{*a} Weimin Zhang^{*a}

^aState Key Laboratory of Applied Microbiology Southern China, Guangdong Provincial Key Laboratory of Microbial Culture Collection and Application, Guangdong Open Laboratory of Applied Microbiology, Guangdong Institute of Microbiology, Guangdong Academy of Sciences, Guangzhou 510070, China

^bSchool of Biosciences and Biopharmaceutics, Guangdong Pharmaceutical University, Guangzhou 510006, China

^cProgram for Natural Products Chemical Biology, Key Laboratory of Plant Resources Conservation and Sustainable Utilization, Guangdong Provincial Key Laboratory of Applied Botany, South China Botanical Garden, Chinese Academy of Sciences, Guangzhou 510650, China

Contents

1. Experimental Section

- 1.1 General experimental procedures
- 1.2 Fungal material and identification
- 1.3 Fermentation, extraction and isolation
- 1.4 Quantum chemical calculation of NMR chemical shifts and ECD spectra
- 1.5 Cytotoxic activity assay

2. NMR, HRESIMS, CD, UV and IR spectra of compounds 1-3

Figure S5. ^1H NMR spectrum (600 MHz, CD_3COCD_3) of **1**

Figure S6. ^{13}C NMR spectrum (150 MHz, CD_3COCD_3) of **1**

Figure S7. ^1H - ^1H COSY spectrum of **1** in CD_3COCD_3

Figure S8. HSQC spectrum of **1** in CD_3COCD_3

Figure S9. HMBC spectrum of **1** in CD_3COCD_3

Figure S10. NOESY spectrum of **1** in CD_3COCD_3

Figure S11. HRESIMS spectrum of **1**

Figure S12. CD spectrum of **1**

Figure S13. UV spectrum of **1**

Figure S14. IR spectrum of **1**

Figure S15. ^1H NMR spectrum (600 MHz, CDCl_3) of **2**

Figure S16. ^{13}C NMR spectrum (150 MHz, CDCl_3) of **2**

Figure S17. ^1H - ^1H COSY spectrum of **2** in CDCl_3

Figure S18. HSQC spectrum of **2** in CDCl_3

Figure S19. HMBC spectrum of **2** in CDCl_3

Figure S20. NOESY spectrum of **2** in CDCl_3

Figure S21. HRESIMS spectrum of **2**

Figure S22. CD spectrum of **2**

Figure S23. UV spectrum of **2**

Figure S24. IR spectrum of **2**

Figure S25. ^1H NMR spectrum (600 MHz, CD_3OD) of **3**

Figure S26. ^{13}C NMR spectrum (150 MHz, CD_3OD) of **3**

1. Experimental Section

1.1 General experimental procedures

IR data were obtained by a Shimadzu IR Affinity-1 spectrometer (Shimadzu, Kyoto, Japan). UV spectra were collected using a Shimadzu UV-2600 spectrophotometer (Shimadzu, Kyoto, Japan). Optical rotations were done with an Anton Paar MCP-500 spectropolarimeter (Anton Paar, Graz, Austria). Circular dichroism (CD) spectra were afforded under N₂ gas by a Jasco 820 spectropolarimeter (Jasco Corporation, Kyoto, Japan). HRESIMS were acquired on a Thermo MAT95XP (Thermo Fisher Scientific, Bremen, Germany). NMR spectra were acquired by a Bruker Avance-600 spectrometer (Bruker, Fällanden, Switzerland). A YMC-pack ODS-A/AQ column (250 × 10 mm, 5 μm, 12 nm, YMC CO., Ltd, Kyoto, Japan) was used for semipreparative HPLC separation. Silica gel (100-200 mesh and 200-300 mesh, Qingdao Marine Chemical Inc., Qingdao, China), C₁₈ reversed-phase silica gel (40–63 μm, Merck, Darmstadt, Germany) and Sephadex LH-20 gel (Pharmacia Fine Chemical Co. Ltd., Uppsala, Sweden) were used in the chromatography processes. Fractions were monitored by TLC and spots were detected on heated TLC plates (silica gel GF₂₅₄ plates, Qingdao Marine Chemical Inc., Qingdao, China) with 10% H₂SO₄ in EtOH under UV light.

1.2 Fungal material and identification

The strain FS441 used in this work was isolated from a sediment sample, which was collected at the depth of 3000 m in the Indian Ocean (88°58.640' E, 0°00.307' S) in April 2016. The sequence data for this strain have been submitted to the GenBank under accession No. MK592793. By using BLAST (nucleotide sequence comparison program) to search the GenBank database, FS441 has 98.9% similarity to *Phomopsis tersa* SYJM09 (Accession No. JF923840). And the strain was preserved at the Guangdong Provincial Key Laboratory of Microbial Culture Collection and Application, Guangdong Institute of Microbiology.

GGGAATGCTGGAGCGCCAGGCGCACCCAGAAACCCTTTGTGAACTTATACCTTACTGT
TGCCTCGGCGTACGCTGGCCCCCAGGGGTCCCTCTGTCTACAGAGGAGCAGGCACGCC
GGCGGCCAAGTTAACTCTTGTTTTTACACTGAACTCTGAGAAAAACAAAAATGAAT
CAAAACTTTCAACAACGGATCTCTTGTTCTGGCATCGATGAAGAACGCAGCGAAATG
CGATAAGTAATGTGAATTGCAGAATTCAGTGAATCATCGAATCTTTGAACGCACATTGC
GCCCTCCGGTATTCCGGAGGGCATGCCTGTTTCGAGCGTCATTCAACCCTCAAGCCTGG

CTTGGTGTGGGGCACTGCTTCTCTCGCGGGAAGCAGGCCCTCAAATCTAGTGGCGAG
 CTCGCCAGGACCCCGAGCGTAGTAGTTAAACCCTCGCTTTGGAAGGCCCTGGCGGTGC
 CCTGCCGTAAACCCCAACTCTTGAAAATTTGACCTCGGATCAGGTAGGAATACCCGC
 TGAACTTAAGCATATCAATAAGCCGGAGGAA

Figure S1. The strain's (*Phomopsis tersa* FS441) ITS sequence of the rDNA (GenBank No. MK592793)

1.3 Fermentation, extraction and isolation

The marine fungus *P. tersa* FS441 was cultured on potato dextrose agar (PDA) at 28°C for 7 days to prepare the seed culture, and then inoculated into flasks (3 L) containing 9 g sea salts, 250 g of rices and 300 mL of waters. After that, all flasks were incubated at 28 °C for one month and the fermented rice substrate was extracted repeatedly with EtOAc. After the evaporation of the solvent, a dark brown solid (177.9 g) was obtained. The crude extract was fractionated by silica gel column chromatography (100-200 mesh) with two gradient systems of increasing polarity (petroleum ether/EtOAc, 10:1→1:1; CH₂Cl₂/CH₃OH, 10:1→0:1) to furnish seven fractions (A-G).

Fraction E (41.8 g) was subjected to C-18 reversed-phase silica gel CC (gradient elution with MeOH-H₂O, 30:70→100:0) to afford fifteen subfractions (E1-E15). Then, E8 was subjected to silica gel CC (CH₂Cl₂-MeOH, 30:1→2:1) to obtain four subfractions (E8.1-E8.4). And E8.1 was further separated by silica gel CC (CH₂Cl₂-MeOH, 40:1→5:1) to get four subfractions (E8.1.1-E8.1.4). Semi-preparative HPLC (MeCN-H₂O, 40:60, 2 mL/min) analysis of E8.1.2 afforded **2** (6.1 mg, *t_R* = 34.8 min). E11 was divided into three subfractions (E11.1-E11.3) by Sephadex LH-20 CC (CH₂Cl₂-MeOH, 1:1). E11.3 was further purified by semi-preparative HPLC (MeCN-H₂O, 75:35, 2 mL/min) to yield thirteen parts (E11.3.1-E11.3.13), semi-preparative HPLC (MeCN-H₂O, 60:40, 2 mL/min) analysis of E11.3.4 afforded **1** (2.9 mg, *t_R* = 40.7 min). Furthermore, **3** (365.7mg) was obtained from E12 followed by silica gel CC (CH₂Cl₂-MeOH, 40:1→1:1).

Phomeroid A (**1**): yellow powders; [α]_D²⁵ +146.1 (*c* 0.08, MeOH). CD (0.29 mg/mL, MeOH): 207 (34.0), 250 (-8.1), 333 (4.6) nm. UV (MeOH) λ_{\max} (log ϵ): 204 (4.51) nm. IR ν_{\max} : 2928, 1717, 1541, 1142, 1098, 988, 841 cm⁻¹. ¹H (600 MHz) and ¹³C (150 MHz) NMR spectral data, see Table 1. HRESIMS: *m/z* 535.2723 [M – H][–] (calcd for C₃₂H₃₉O₇, 535.2701).

Phomeroid B (**2**): yellow powders; [α]_D²⁵ +94.3 (*c* 0.11, MeOH). CD (0.32 mg/mL, MeOH): 214

(23.0), 240 (9.7), 263 (-4.6) nm. UV (MeOH) λ_{max} (log ϵ): 253 (4.55), 361 (3.93) nm. IR ν_{max} : 2953, 1755, 1435, 1152, 1084, 733 cm^{-1} . ^1H (600 MHz) and ^{13}C (150 MHz) NMR spectral data, see Table 2. HRESIMS: m/z 595.2906 $[\text{M} + \text{H}]^+$ (calcd for $\text{C}_{32}\text{H}_{43}\text{O}_9$, 595.2902).

1.4 Quantum chemical calculation of NMR chemical shifts and ECD spectra

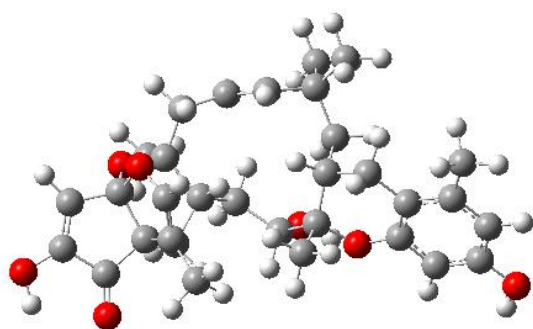
Methods.

MMFF and DFT/TD-DFT calculations were carried out using the Spartan'14 software (Wavefunction Inc., Irvine, CA, USA) and the Gaussian 09 program, respectively.¹ Conformers that had an energy window lower the 5 $\text{kcal}\cdot\text{mol}^{-1}$ were generated and optimized using DFT calculations at the b3lyp/6-31+g (d, p) level. Frequency calculations were performed at the same level to confirm that each optimized conformer was true minimum and to estimate their relative thermal free energy (ΔG) at 298.15 K. Conformers with the Boltzmann distribution over 2% were chosen for ^{13}C -NMR and ECD calculations at mPW1PW91/6-311+g (d, p) and b3lyp/6-311+g (d, p) level, respectively. Additionally, solvent effects were considered based on the self-consistent reaction field (SCRF) method with the polarizable continuum model (PCM).² The ECD spectrum was generated by the SpecDis program³ using a Gaussian band shape with 0.22 eV exponential half-width from dipole-length dipolar and rotational strengths. The DP4⁺ probability simulations were conducted using an applet available at <http://www-jmg.ch.cam.ac.uk/tools/nmr/DP4/>.

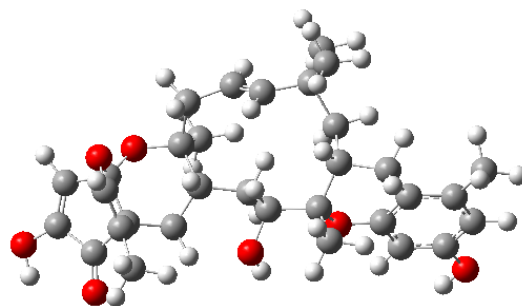
Results.

Table S1. Energy analysis for the Conformers of **1a**.

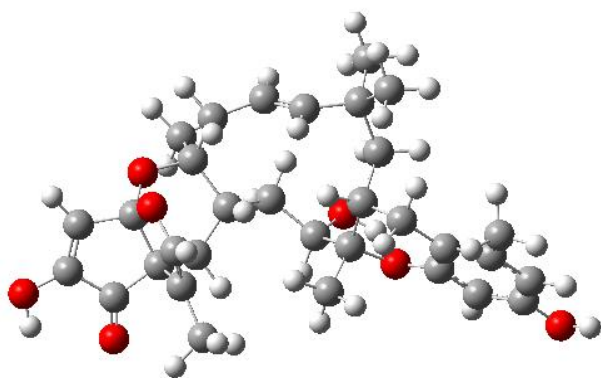
Compound	Conformation	E (Hartree)	E (Kcal/mol)	ΔE (Kcal/mol)	Boltzmann Dist (%)
1a	1a-1	-1770.08622458	-1110734.239	0	47.41%
	1a-2	-1770.08360417	-1110732.595	1.644314874	2.95%
	1a-3	-1770.08621137	-1110734.231	0.008289313	46.75%
	1a-4	-1770.08358758	-1110732.584	1.654725147	2.90%



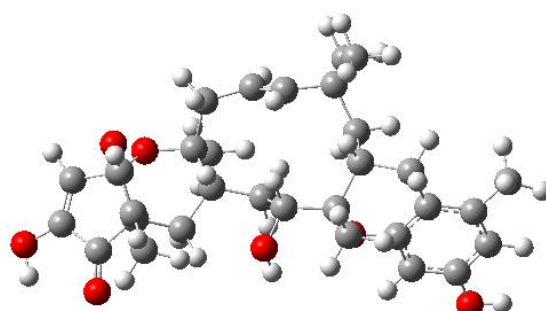
1a-1



1a-2



1a-3

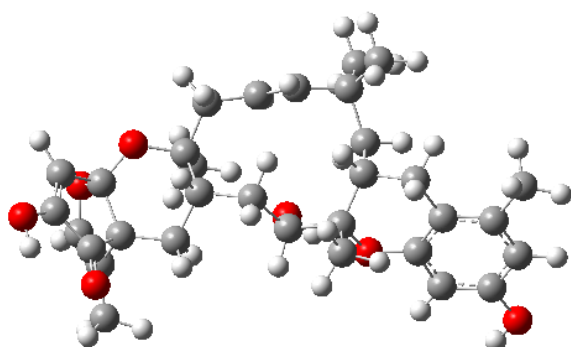


1a-4

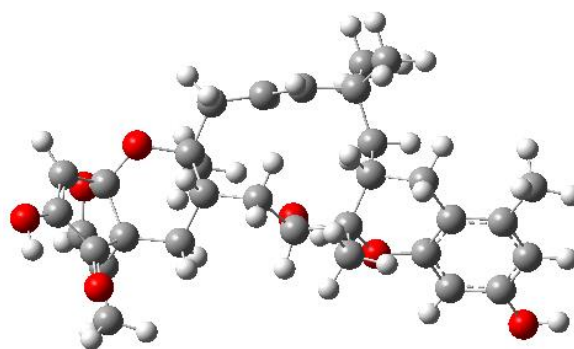
Figure S2. B3LYP/6-31+G (d,p) optimized low-energy conformers of **1a**

Table S2. Energy analysis for the Conformers of **1b**.

Compound	Conformation	E (Hartree)	E (Kcal/mol)	ΔE (Kcal/mol)	Boltzmann Dist (%)
1b	1b-1	-1770.08384429	-1110732.746	0.0433981	48.17%
	1b-2	-1770.08391345	-1110732.789	0	51.83%



1b-1



1b-2

Figure S3. B3LYP/6-31+G (d,p) optimized low-energy conformers of **1b**

Table S3. Energy analysis for the Conformers of **2**.

Compound	Conformation	E (Hartree)	E (Kcal/mol)	ΔE (Kcal/mol)	Boltzmann Dist (%)
2	2-1	-1997.88237883	-1253676.987	0	51.79%
	2-2	-1997.88130745	-1253676.314	0.672294057	16.64%
	2-3	-1997.88130753	-1253676.314	0.672243857	16.64%
	2-4	-1997.88095746	-1253676.095	0.891913797	11.48%
	2-5	-1997.87982119	-1253675.382	1.604926517	3.44%

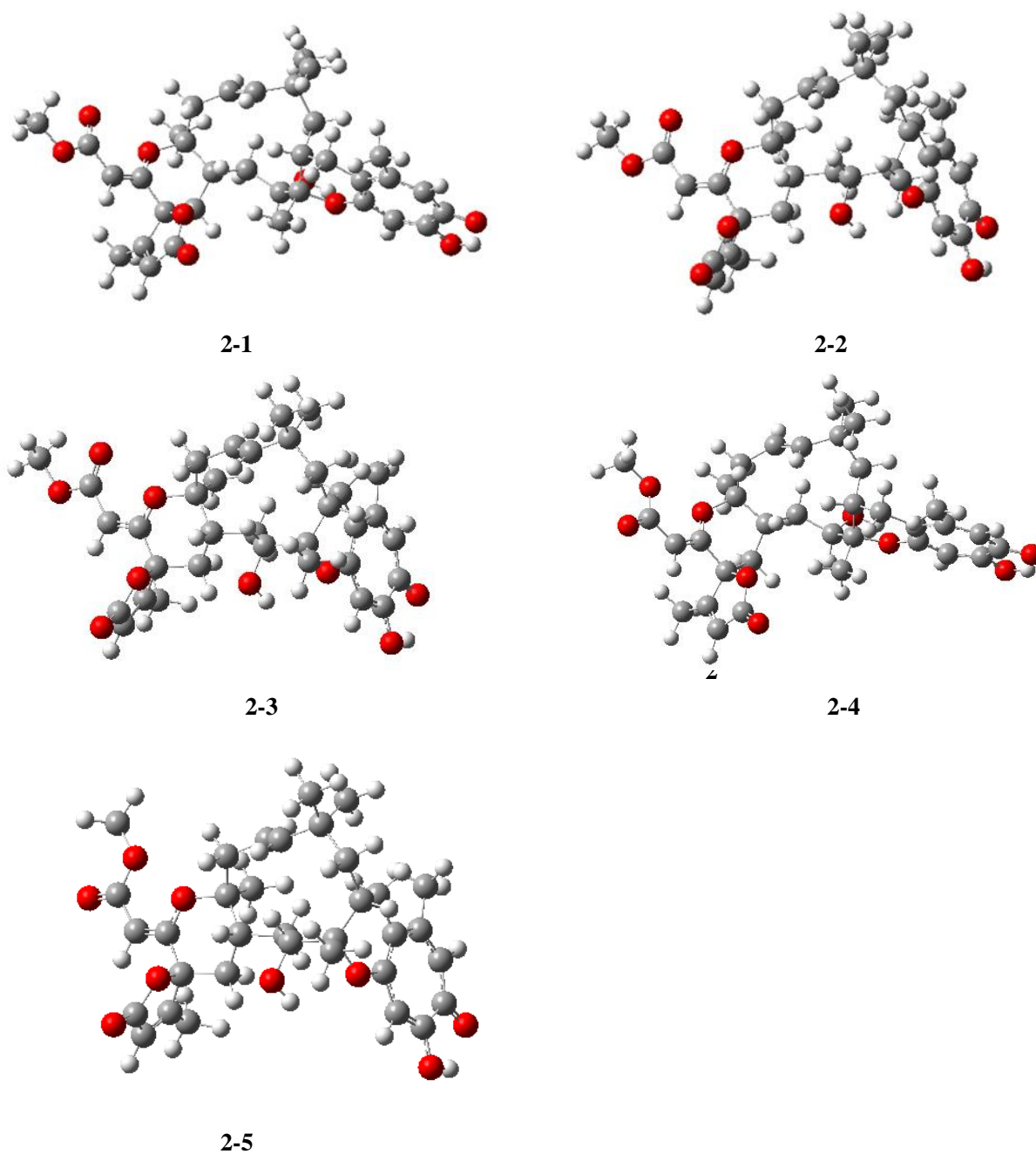


Figure S4. B3LYP/6-31+G (d,p) optimized low-energy conformers of **2**

1.5 Cytotoxic activity assay

Compounds **1-3** were evaluated for their cytotoxic activity against SF-268, MCF-7, HepG-2, A549 cell lines by using the SRB method.⁴ The cells (180 μ L) with a density of 3×10^4 cells/mL of media on 96-well plate were put under 37 $^{\circ}$ C at 5% CO₂ condition and incubated for 24 h. Then, 20 μ L of various concentrations of compounds were added and further incubated for 72 h. After that, the cell monolayers were fixed by 50% (wt/v) trichloroacetic acid (50 μ L) and stained for 30 min by 0.4% (wt/v) SRB, which was dissolved in 1% acetic acid. The unbound dye was removed by washing repeatedly with 1% acetic acid, and then dissolved into the protein-bound dye in 10 mM Tris base solution (200 μ L) for OD determination at 570 nm using a microplate reader. Adriamycin was used as a positive control possessing potent cytotoxic activity. All data were obtained in triplicate, and the IC₅₀ values were calculated by the SigmaPlot 10.0 software (Systat Software Inc., San Jose, California, America) with the use of a non-linear curve-fitting method. The SF-268, MCF-7, HepG-2, A549 cell lines were provided by the Chinese Academy of Sciences Cell Bank.

References

- 1 M. J. Frisch, G. W. Trucks, H. B. Schlegel, G. E. Scuseria, M. A. Robb, J. R. Cheeseman, G. Scalmani, V. Barone, B. Mennucci, G. A. Petersson, H. Nakatsuji, M. Caricato, X. Li, H. P. Hratchian, A. F. Izmaylov, J. Bloino, G. Zheng, J. L. Sonnenberg, M. Hada, M. Ehara, K. Toyota, R. Fukuda, J. Hasegawa, M. Ishida, T. Nakajima, Y. Honda, O. Kitao, H. Nakai, T. Vreven, J. A. Montgomery Jr., J. E. Peralta, F. Ogliaro, M. Bearpark, J. J. Heyd, E. Brothers, K. N. Kudin, V. N. Staroverov, R. Kobayashi, J. Normand, K. Raghavachari, A. Rendell, J. C. Burant, S. S. Iyengar, J. Tomasi, M. Cossi, N. Rega, J. M. Millam, M. Klene, J. E. Knox, J. B. Cross, V. Bakken, C. Adamo, J. Jaramillo, R. Gomperts, R. E. Stratmann, O. Yazyev, A. J. Austin, R. Cammi, C. Pomelli, J. W. Ochterski, R. L. Martin, K. Morokuma, V. G. Zakrzewski, G. A. Voth, P. Salvador, J. J. Dannenberg, S. Dapprich, A. D. Daniels, Ö. Farkas, J. B. Foresman, J. V. Ortiz, J. Cioslowski, D. J. Fox, Gaussian 09, revision D.01, Gaussian, Inc., Wallingford, CT, 2013.
- 2 P. Wu, J. Xue, L. Yao, L. Xu, H. Li and X. Wei, *Org. Lett.*, 2015, **17**, 4922-4925.
- 3 T. Bruhn, A. Schaumlöffel, Y. Hemberger and G. Bringmann, *Chirality*, 2013, **25**, 243-249.
- 4 P. Skehan, R. Storeng, D. Scudiero, A. Monks, J. McMahon, D. Vistica, J. T. Warren, H. Bokesch, S. Kenney and M. R. Boyd, *J. Natl. Cancer. Inst.*, 1990, **82**, 1107-1112.

2. NMR, HRESIMS, CD, UV and IR spectrum of compounds 1-3

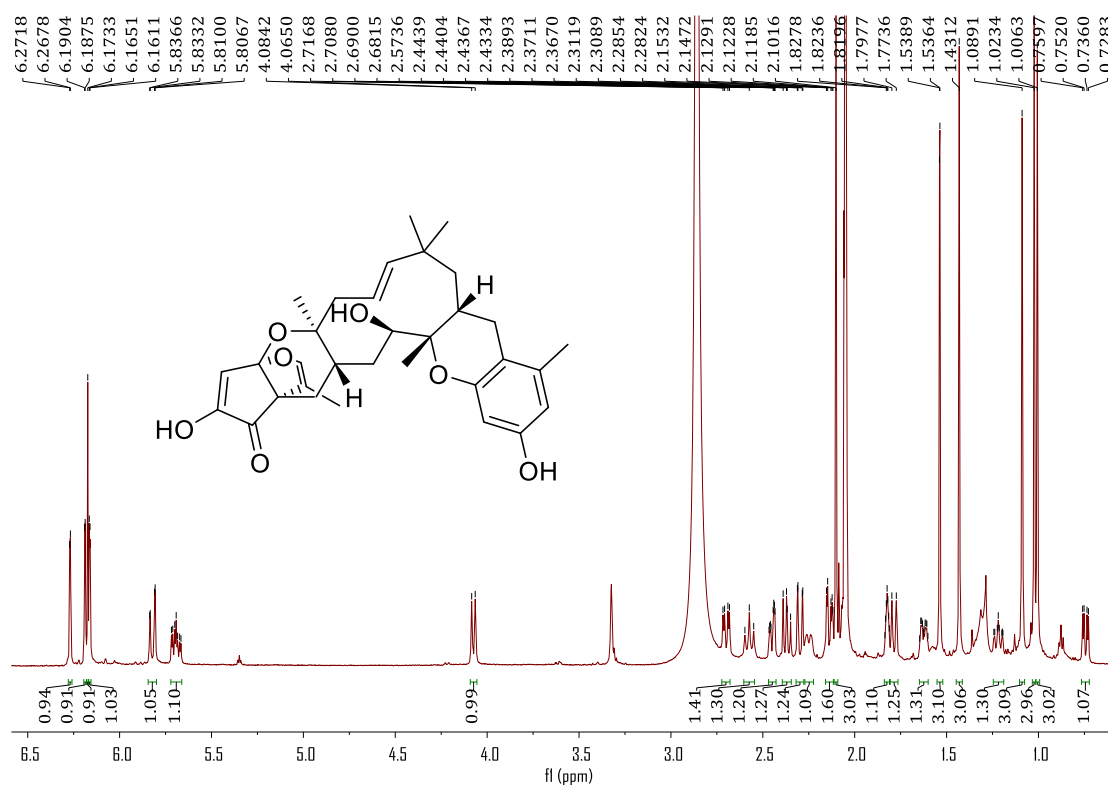


Figure S5. ¹H NMR spectrum (600 MHz, CD₃COCD₃) of 1

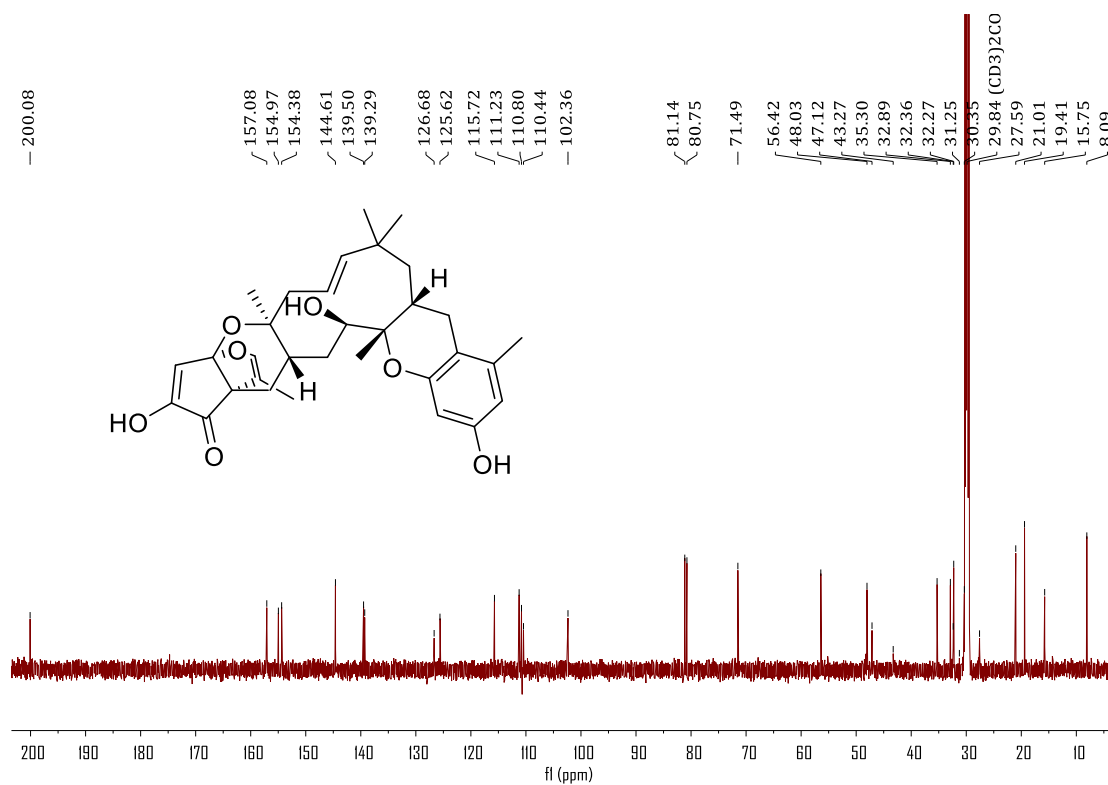


Figure S6. ¹³C NMR spectrum (150 MHz, CD₃COCD₃) of 1

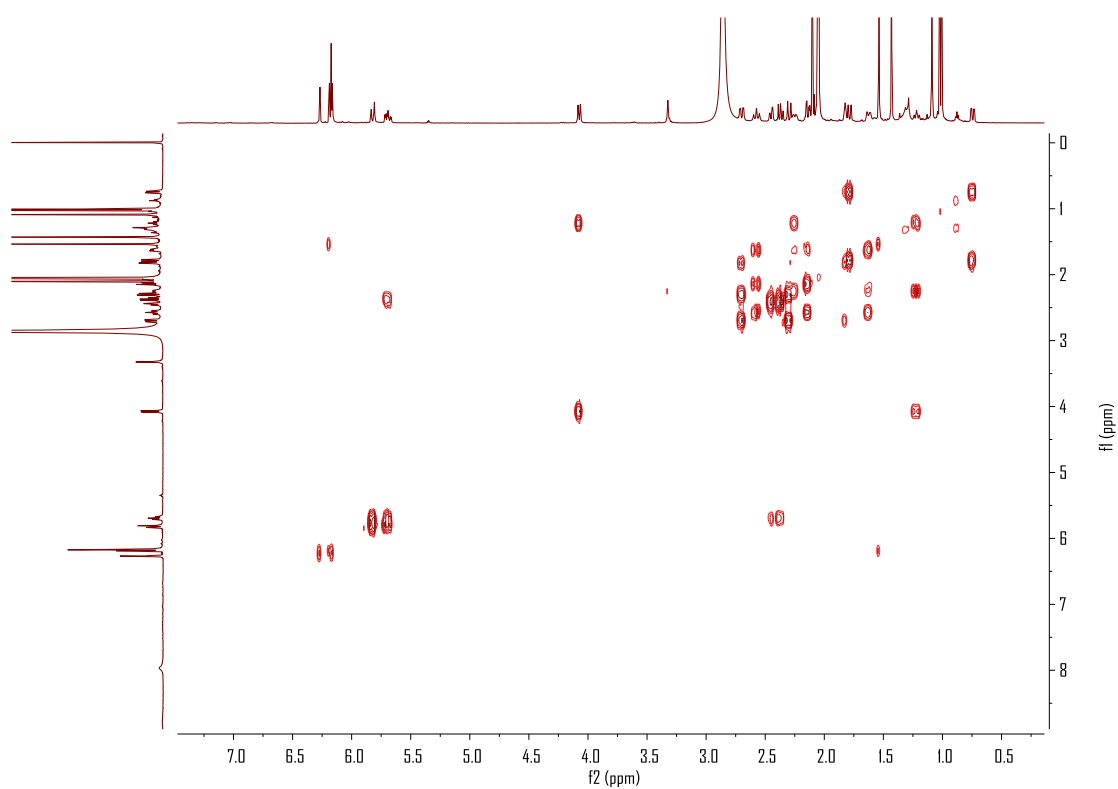


Figure S7. ^1H - ^1H COSY spectrum of **1** in CD_3COCD_3

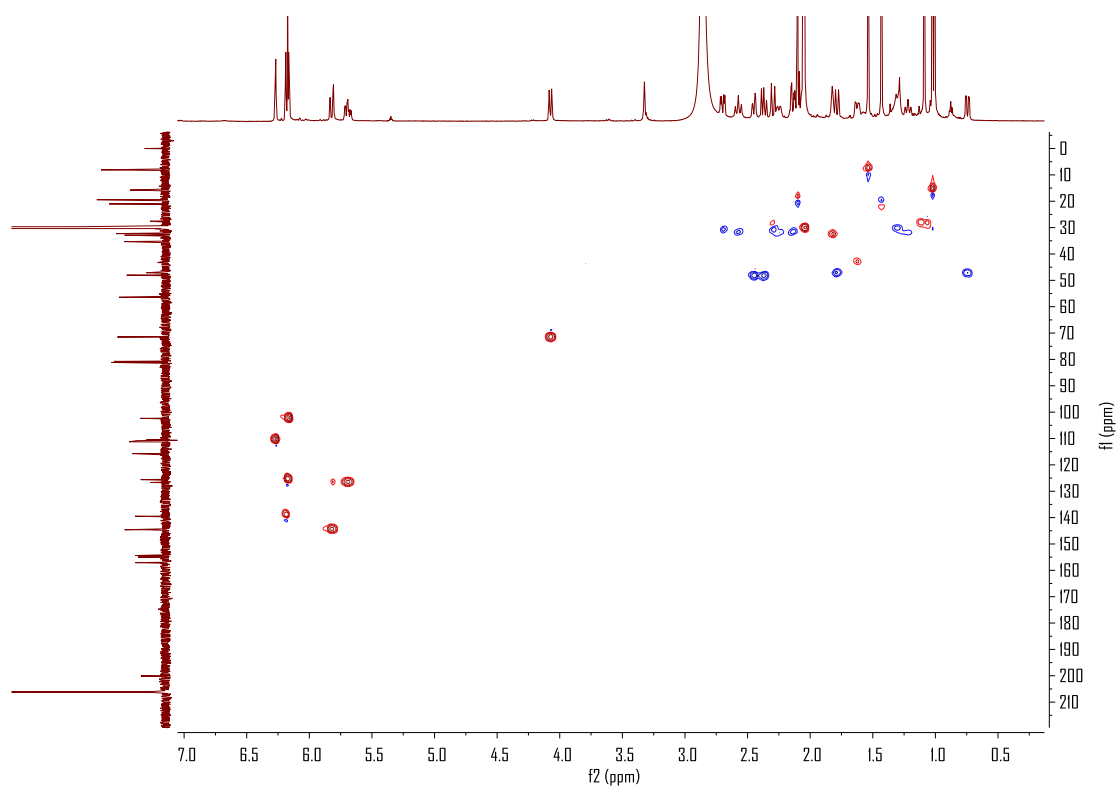


Figure S8. HSQC spectrum of **1** in CD_3COCD_3

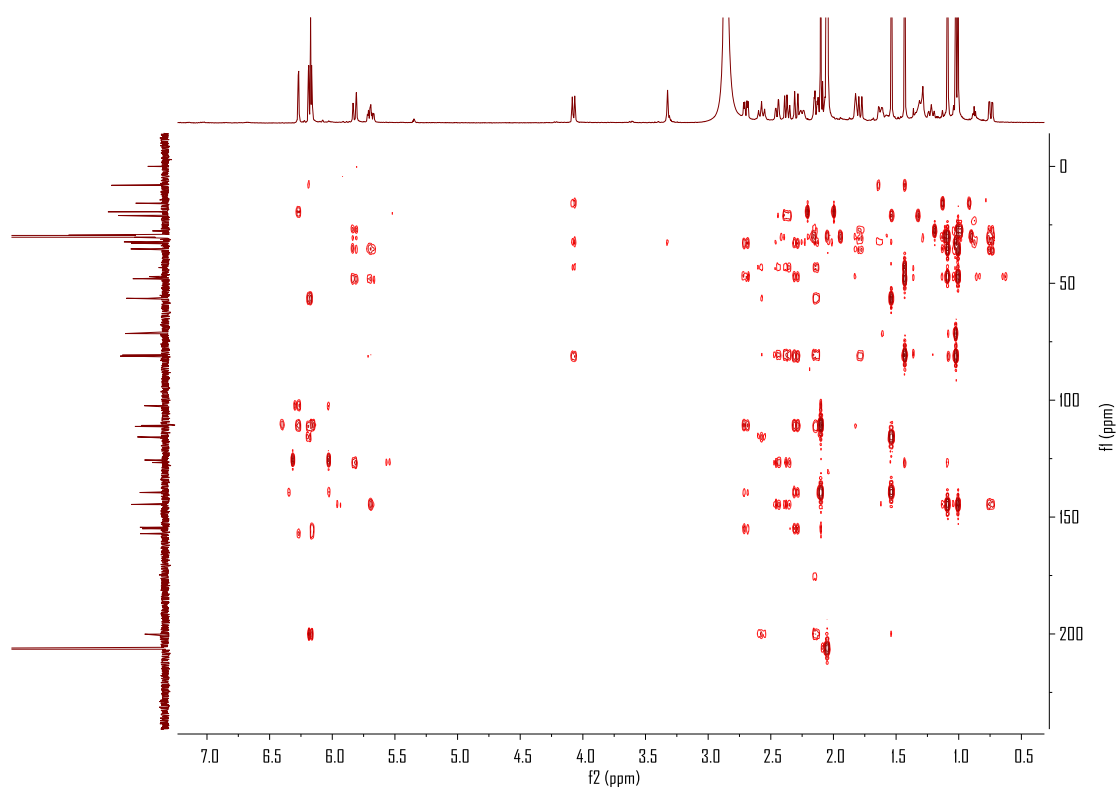


Figure S9. HMBC spectrum of **1** in CD_3COCD_3

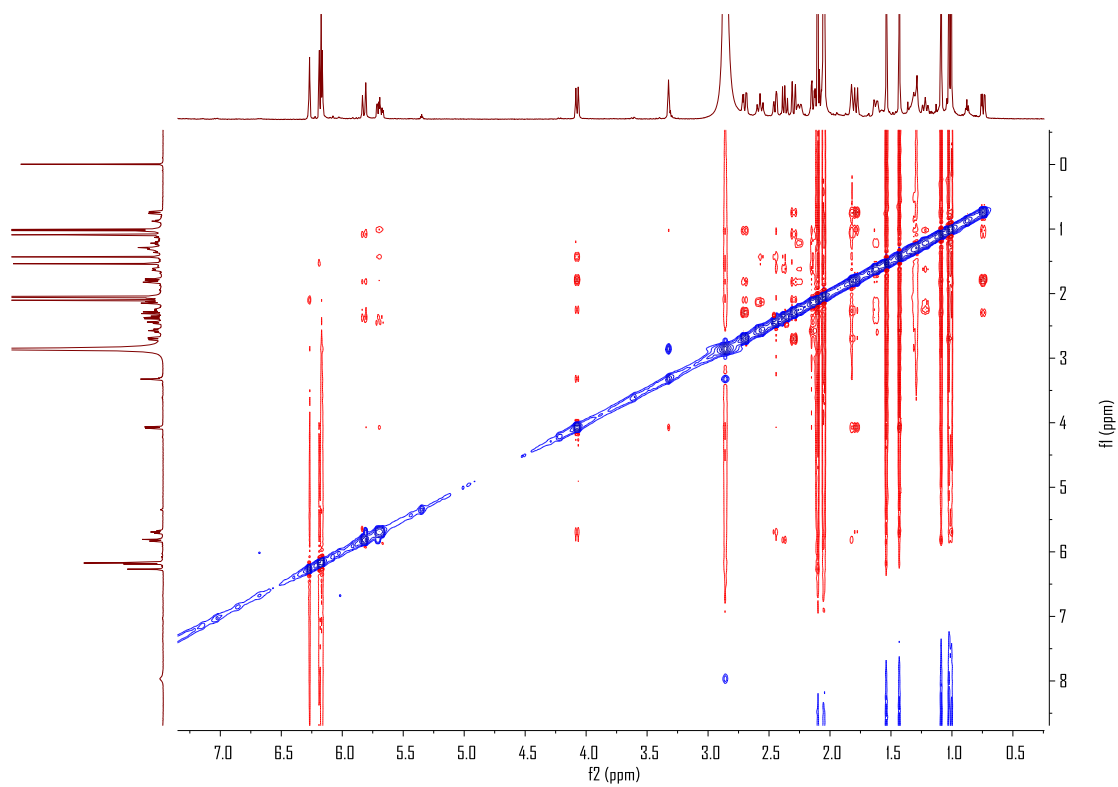


Figure S10. NOESY spectrum of **1** in CD_3COCD_3

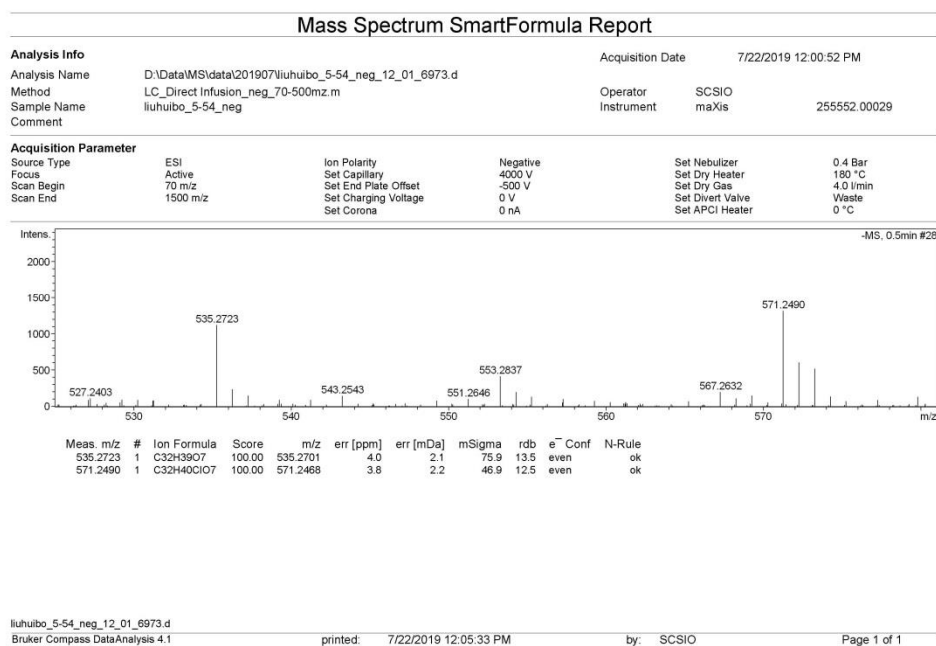


Figure S11. HRESIMS spectrum of **1**

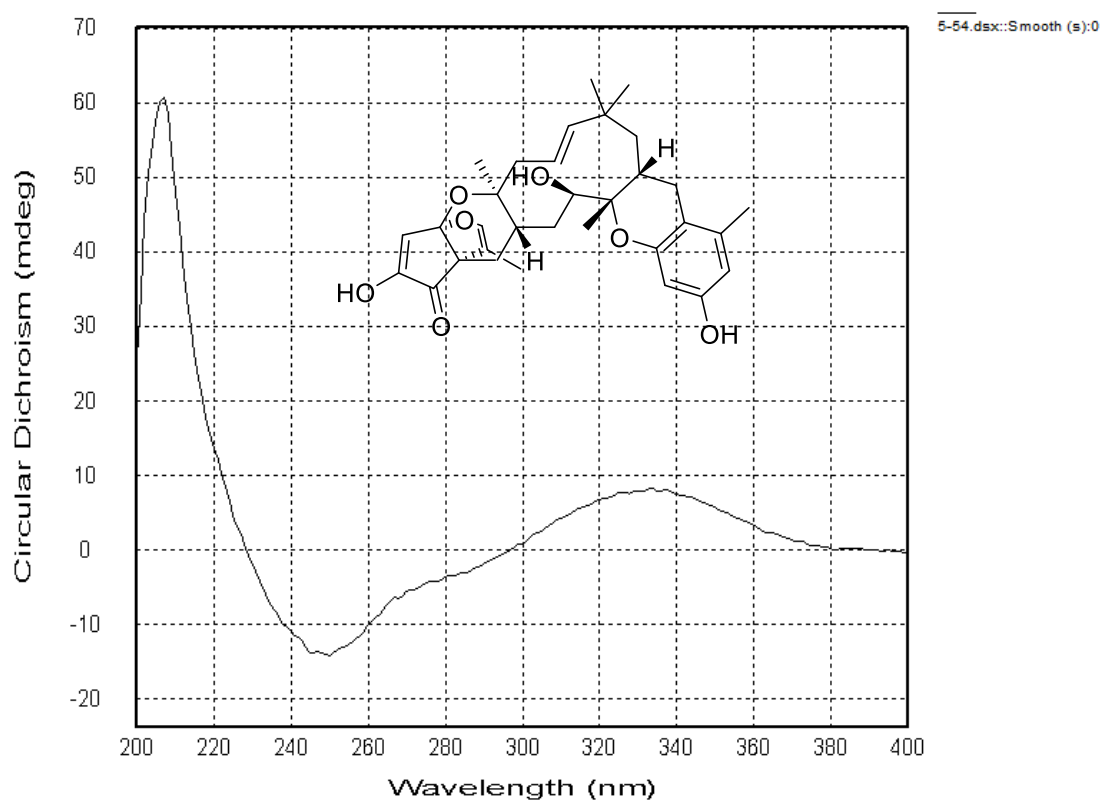
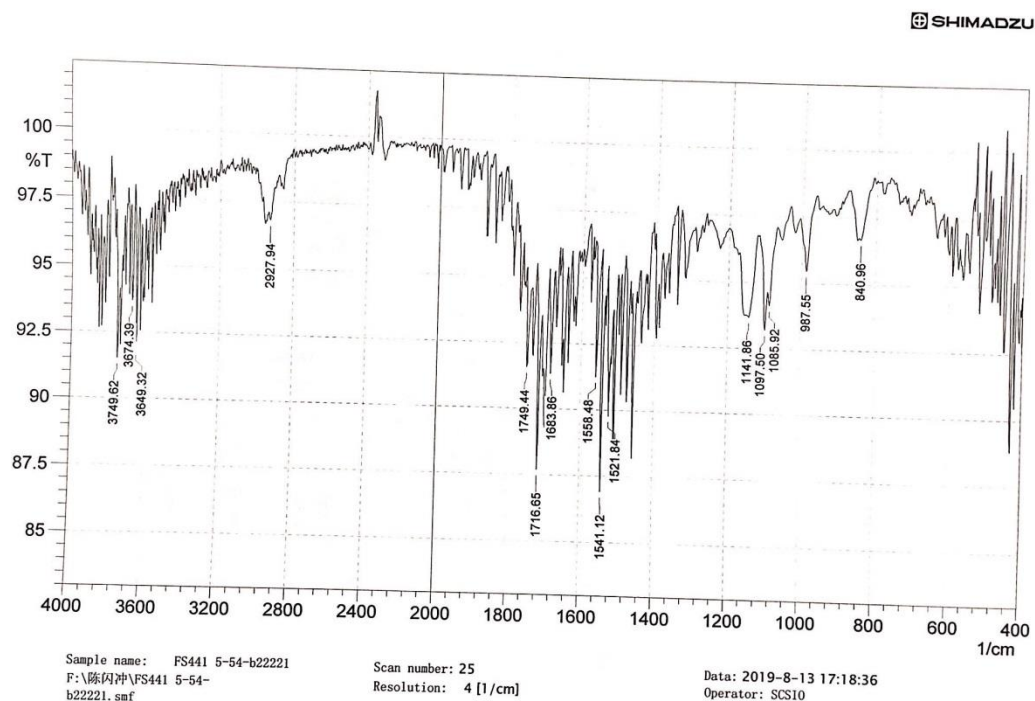
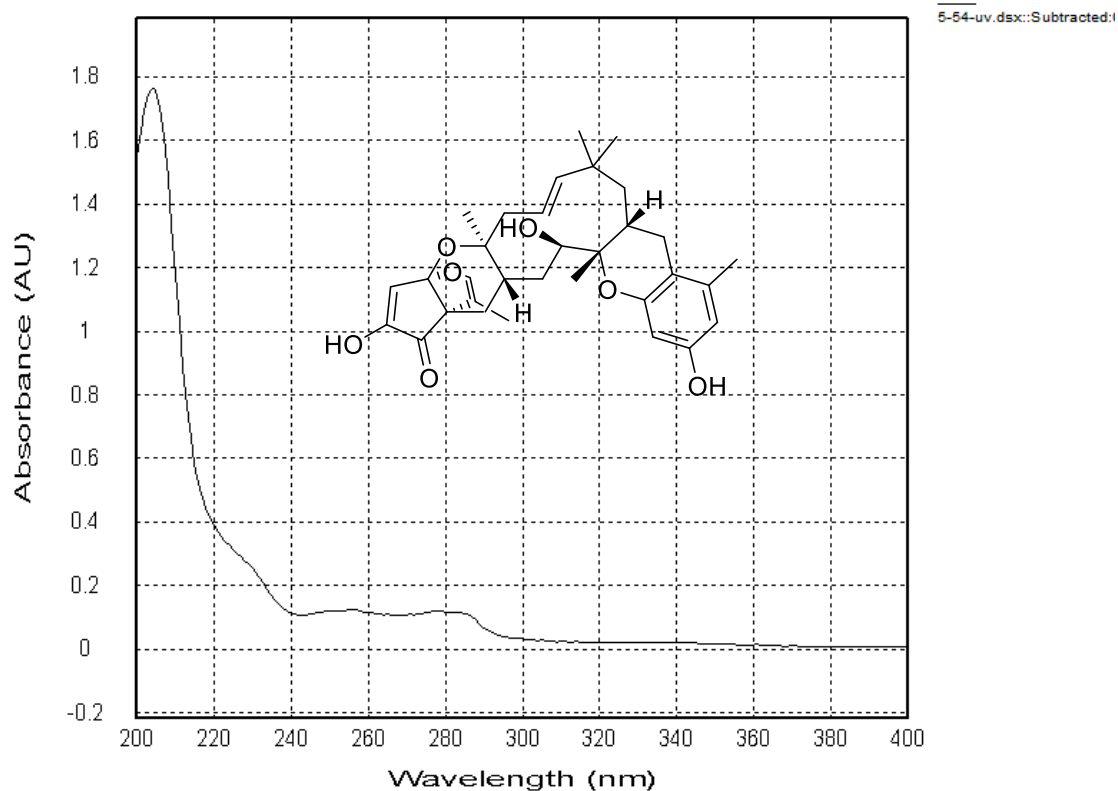


Figure S12. CD spectrum of **1**



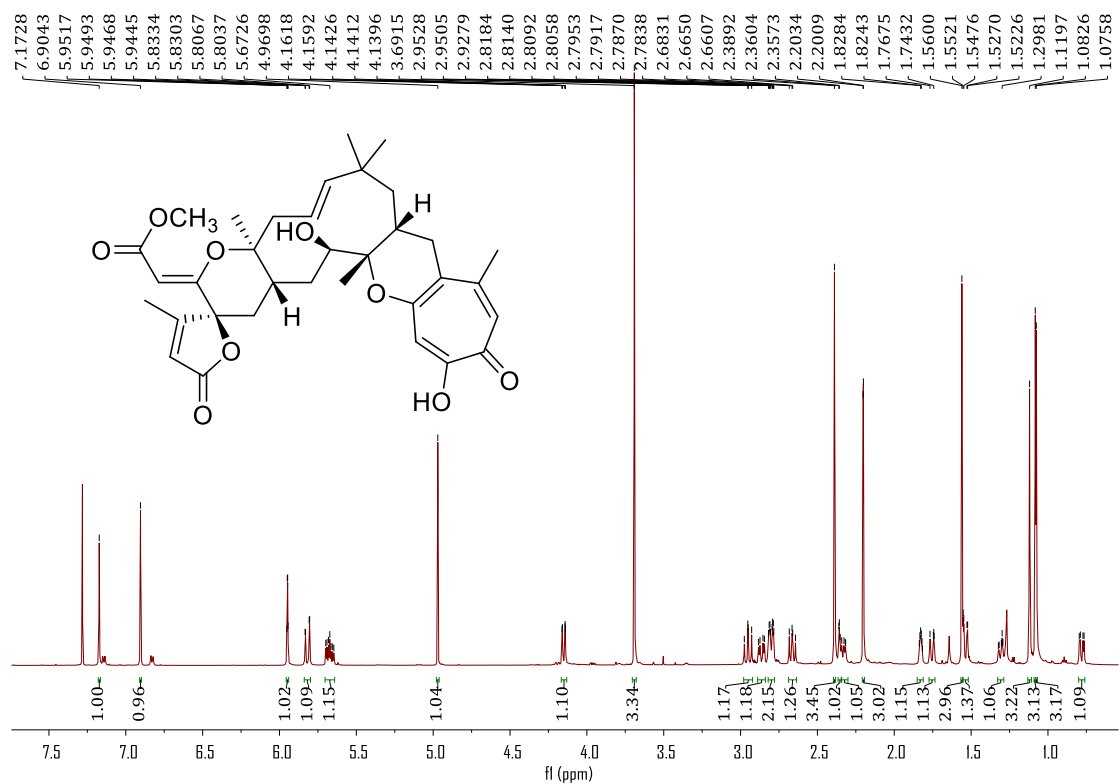


Figure S15. ¹H NMR spectrum (600 MHz, CDCl₃) of **2**

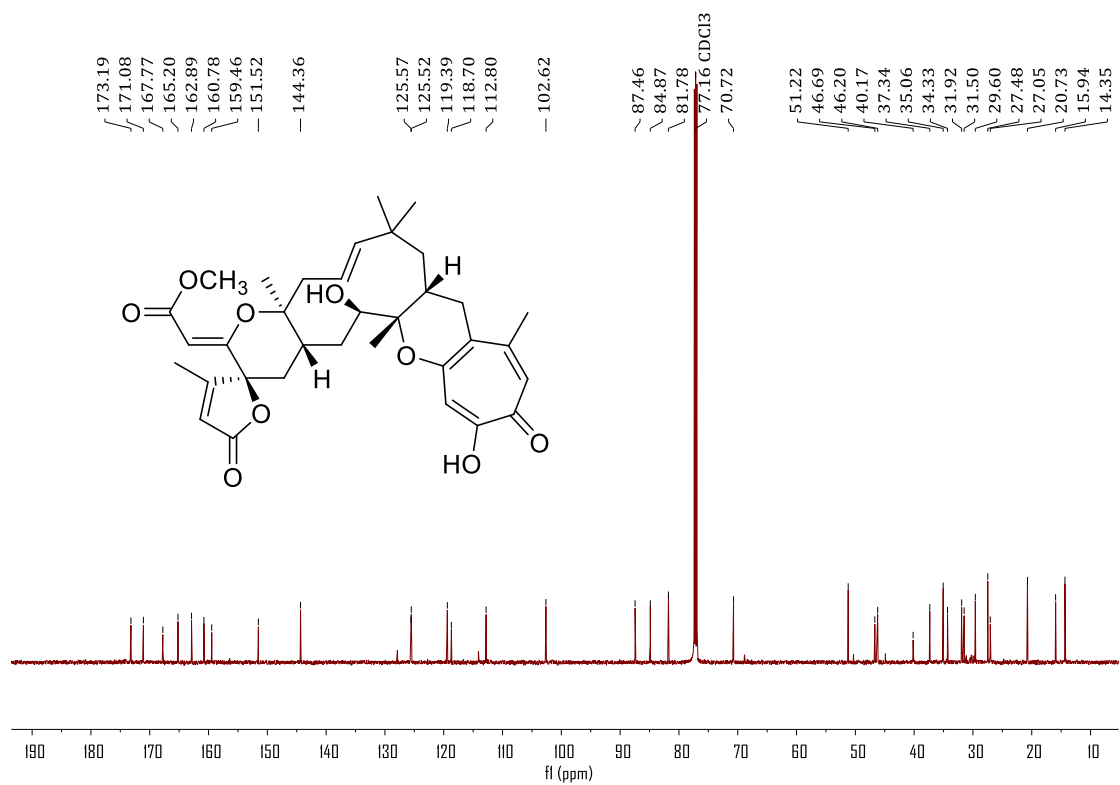


Figure S16. ¹³C NMR spectrum (150 MHz, CDCl₃) of **2**

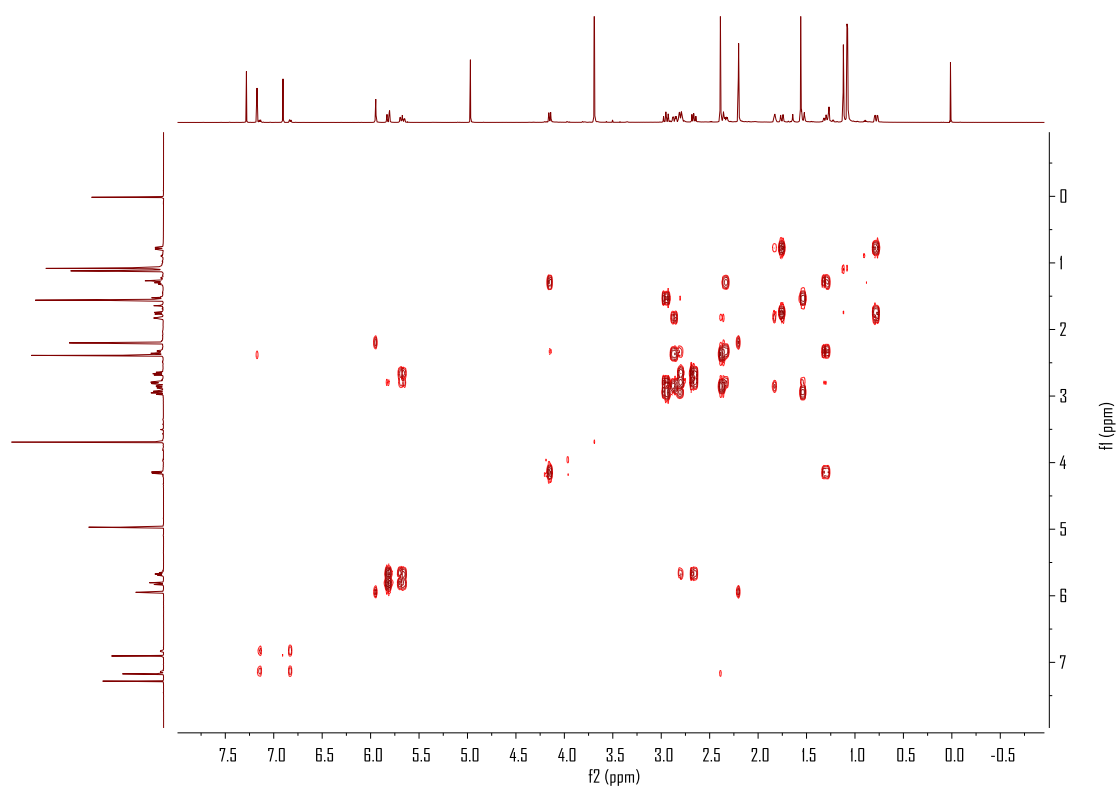


Figure S17. ^1H - ^1H COSY spectrum of **2** in CDCl_3

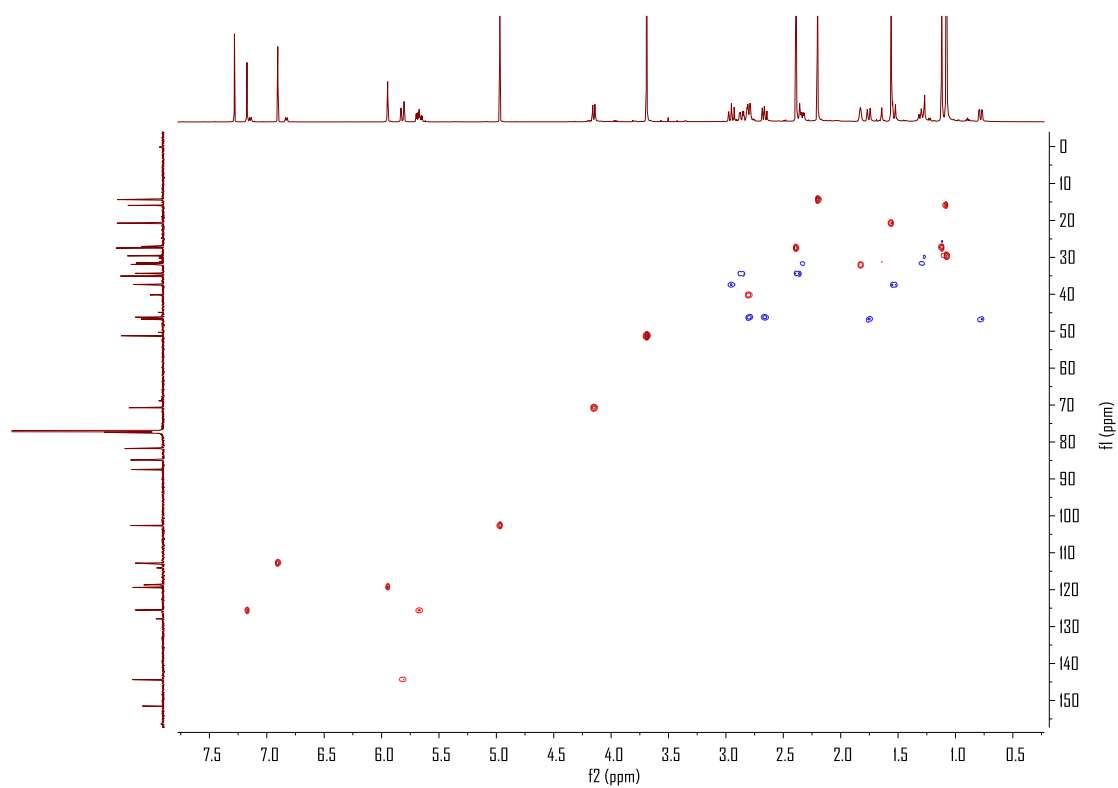


Figure S18. HSQC spectrum of **2** in CDCl_3

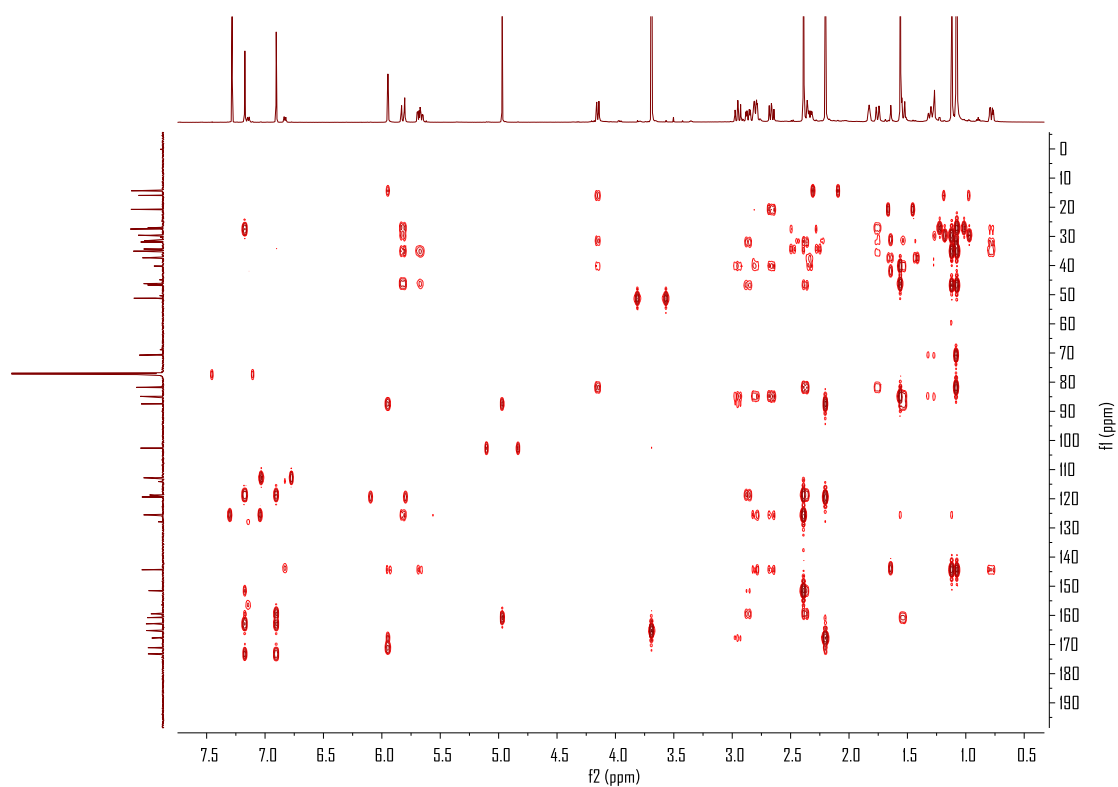


Figure S19. HMBC spectrum of **2** in CDCl₃

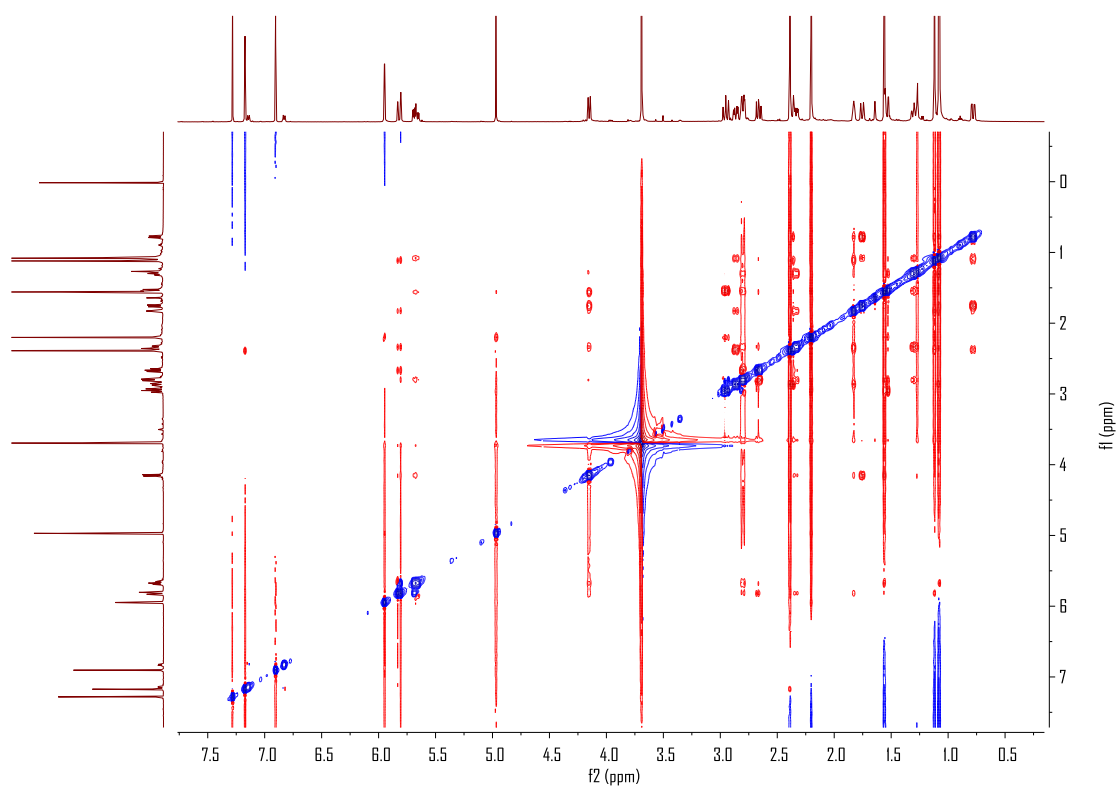


Figure S20. NOESY spectrum of **2** in CDCl₃

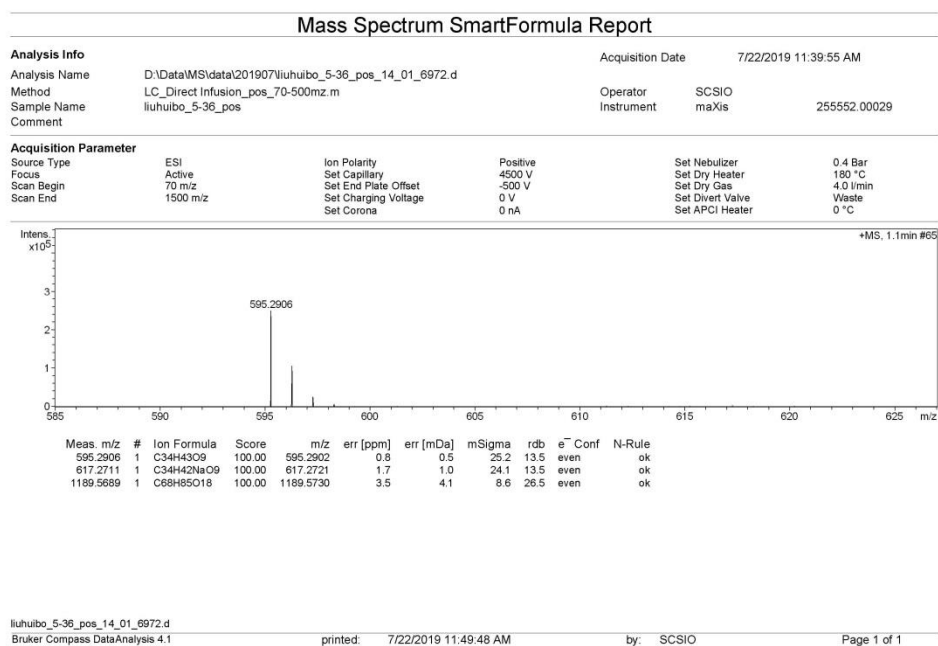


Figure S21. HRESIMS spectrum of **2**

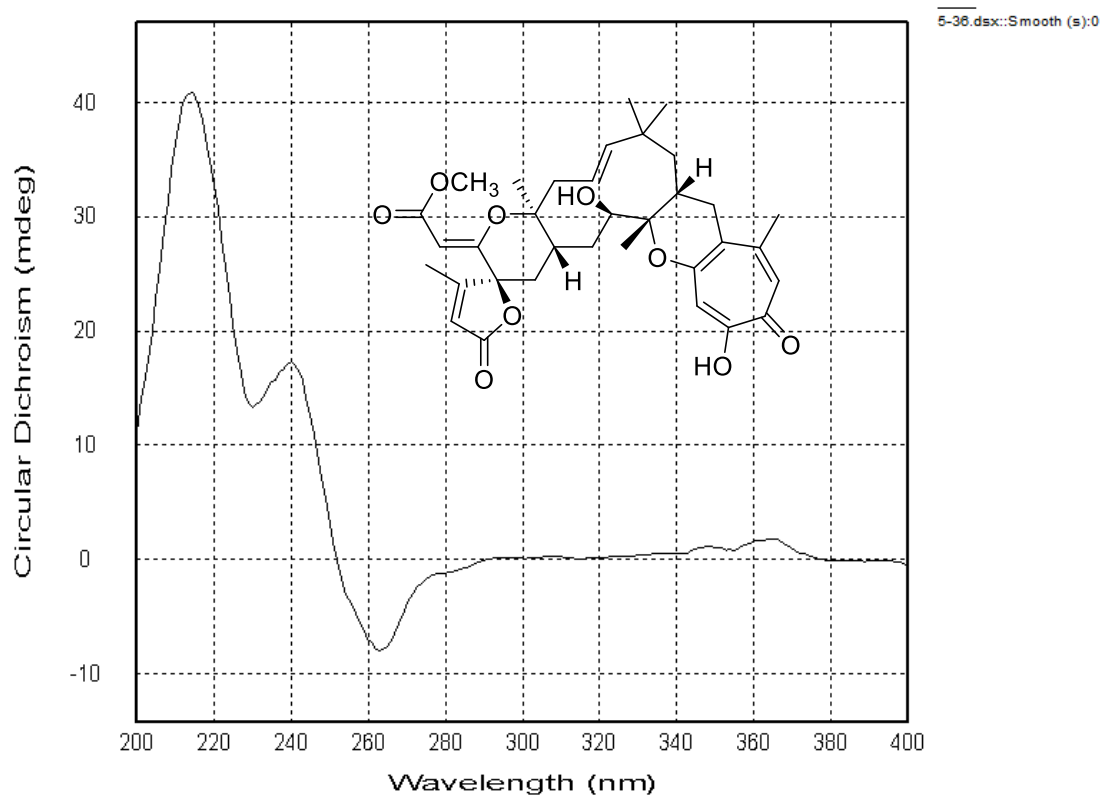
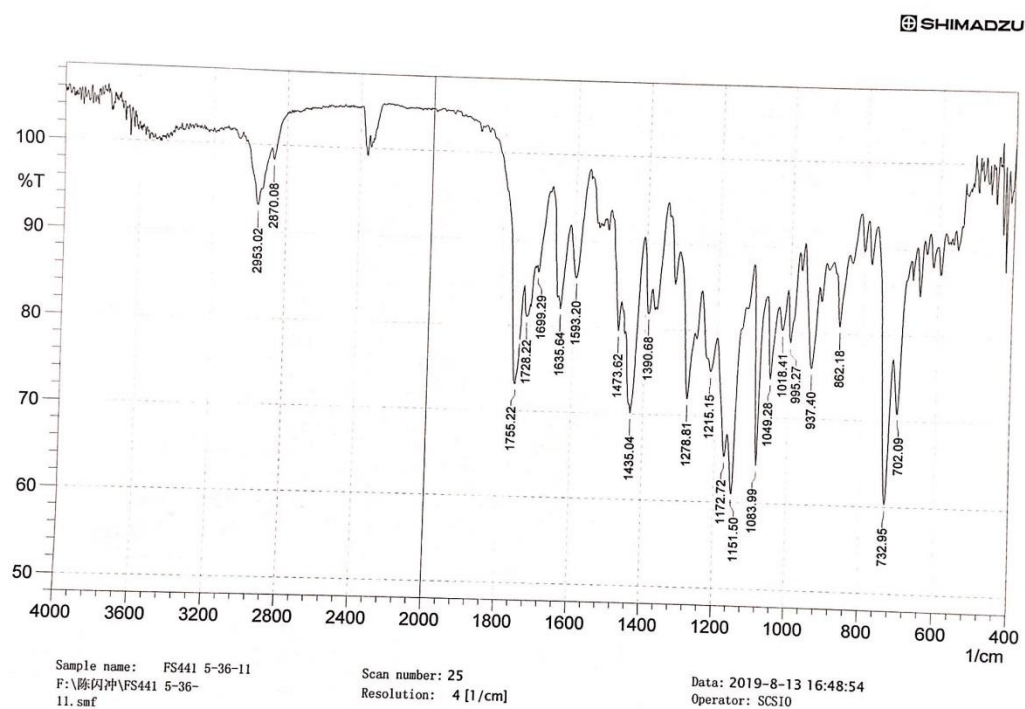
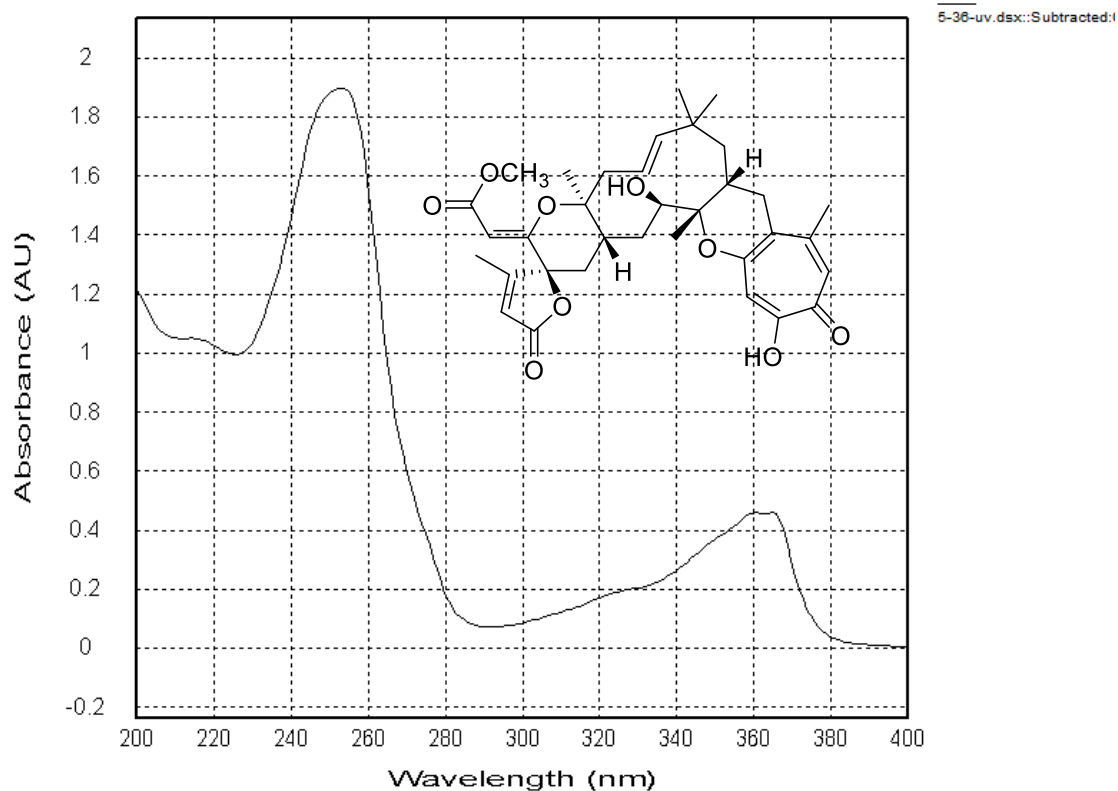


Figure S22. CD spectrum of **2**



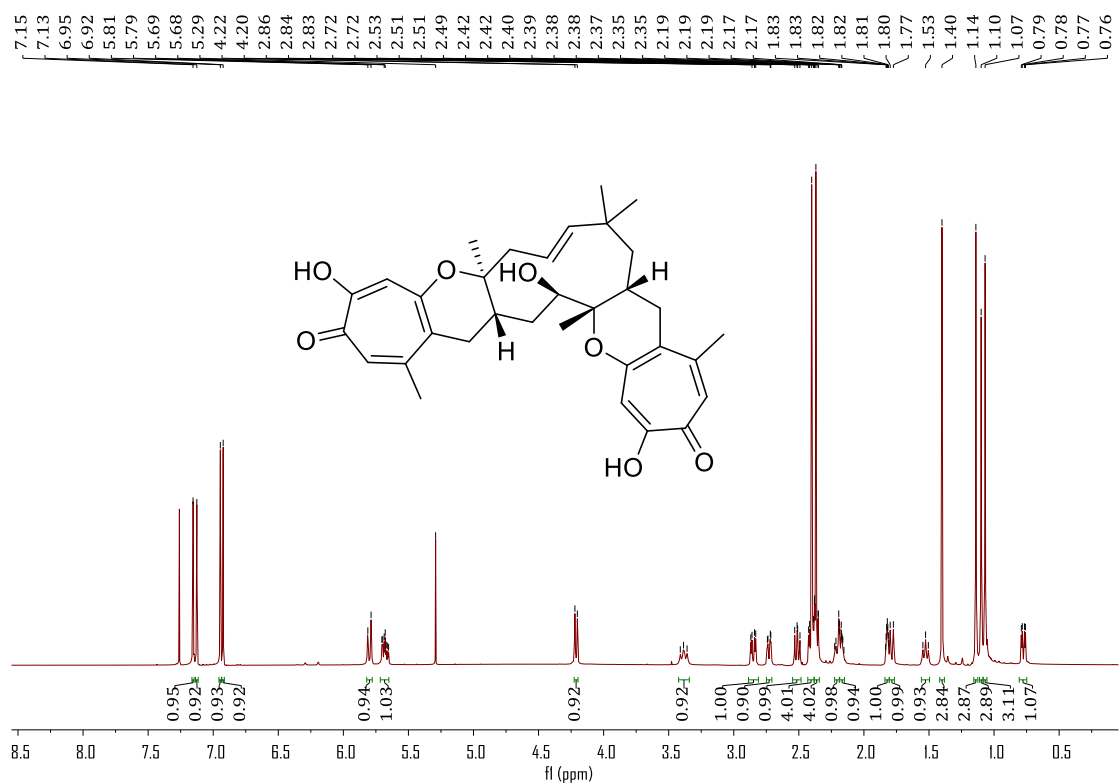


Figure S25. ¹H NMR spectrum (600 MHz, CDCl₃) of **3**

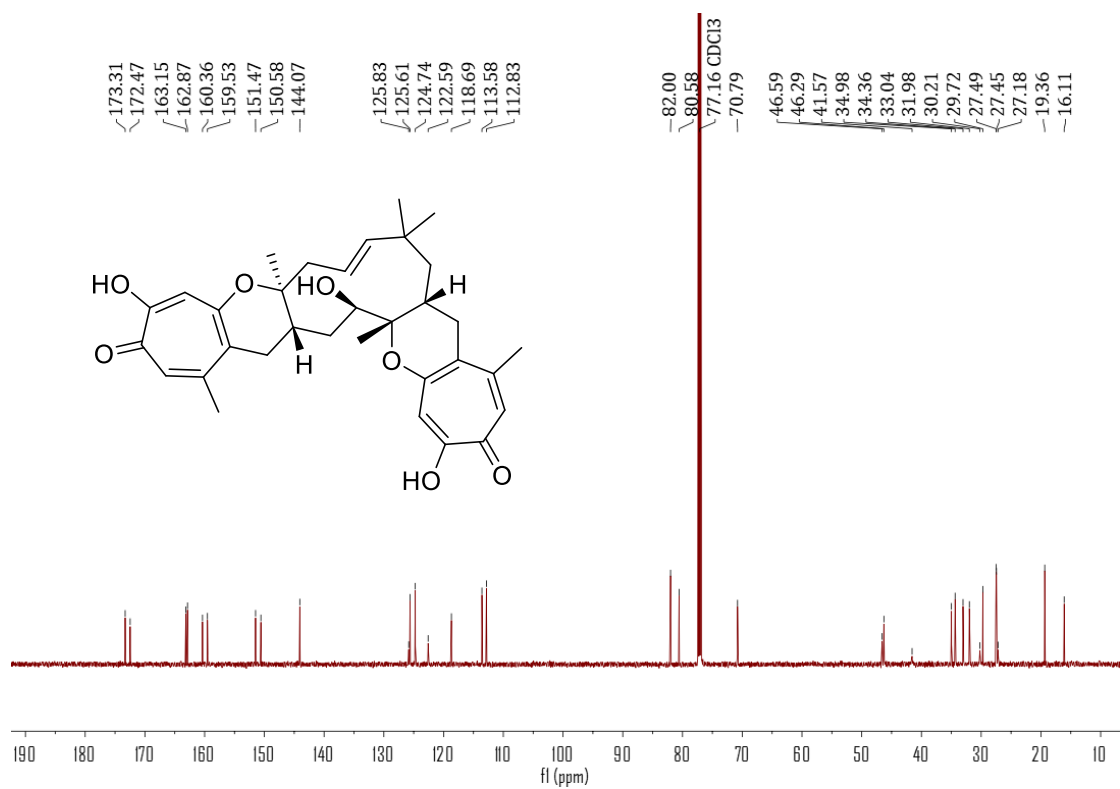


Figure S26. ¹³C NMR spectrum (150 MHz, CDCl₃) of **3**